UNIVERSITYOF
BIRMINGHAM

Research at Birmingham

Comparison of particle velocity measurement techniques in a fluidized bed operating in the square-nosed slugging flow regime

Tebianian, Sina; Dubrawski, Kristian; Ellis, Naoko; Cocco, Ray A.; Hays, Roy; Reddy Karri, S.b.; Leadbeater, Thomas; Parker, David; Chaouki, Jamal; Jafari, Rouzbeh; Garcia-trinanes, Pablo; Seville, Jonathan P.k.; Grace, John R.

Link to publication on Research at Birmingham portal

Download date: 01. Feb. 2019

Accepted Manuscript

Comparison of particle velocity measurement techniques in a fluidized bed operating in the square-nosed slugging flow regime

Sina Tebianian, Kristian Dubrawski, Naoko Ellis, Ray A. Cocco, Roy Hays, S.B. Reddy Karri, Thomas W. Leadbeater, David J. Parker, Jamal Chaouki, Rouzbeh Jafari, Pablo Garcia-Trinanes, Jonathan P.K. Seville, John R. Grace

Comparison of particle velocity measurement techniques in a fluidized bed operating in the square-nosed slugging flow regime

Sina Tebianian[1,*], Kristian Dubrawski[1], Naoko Ellis[1], Ray A. Cocco[2], Roy Hays[2], S.B. Reddy Karri[2], Thomas W. Leadbeater[3], David J. Parker[3], Jamal Chaouki[4], Rouzbeh Jafari[4], Pablo Garcia-Trinanes[5], Jonathan P. K. Seville[5] and John R. Grace[1]

[1] *Department of Chemical and Biological Engineering, University of British Columbia, Vancouver, Canada V6T 1Z3*

[2] *Particulate Solid Research, Inc. Chicago, IL, 60632 United States*

[3] *Positron Imaging Centre, University of Birmingham, Birmingham, B15 2TT United Kingdom*

[4] *Département de génie chimique, Ecole Polytechnique, Montréal, QC, Canada H3T 1J4*

[5] *Department of Chemical and Process Engineering, University of Surrey, Guildford, Surrey GU2 7XH, United Kingdom*

Abstract

The novel "travelling fluidized bed" (TFB), operated under identical conditions, was deployed to compare alternate experimental measurement techniques for the investigation of solid motion in gas-fluidized beds operating in the square-nosed slugging regime. Measurements of particle velocity obtained by radioactive particle tracking (RPT − non-invasive at the Ecole Polytechnique de Montréal), positron emission particle tracking (PEPT − non-invasive at University of Birmingham), optical fibre probes (invasive at UBC) and borescopic high speed particle image velocimetry (invasive at PSRI) are compared for sand particles of mean diameter 292 μm. Significant differences between the time-average radial profiles of particle velocity are observed in many cases. The results provide valuable insights on the merits and challenges of advanced particle velocity measurement techniques.

Keywords: Fluidization; Square-nosed slugging; Particle velocity; Optical probes; Particle tracking; Borescopy

---

[*] Corresponding author, Email: sinatebian@gmail.com, Phone: (604)8223121

1.   Introduction

Among the hydrodynamic features characterizing gas-fluidized beds, particle velocity represents a key parameter which influences heat transfer, gas-solids mixing, erosion, attrition, solids entrainment and particle flux [1].

Various techniques have been investigated for measuring particle velocity in gas-fluidized beds using invasive and non-invasive methods [2]. Invasive techniques based on probing methods represent a good candidate for monitoring plant performance and process optimization in industrial units. However, the degree of flow interference from the probes must be quantified by direct comparison with other techniques employed on the same equipment under identical operating conditions [1,3]. Reliability of non-invasive particle tracking techniques for representing the solid motion should also be investigated. Direct comparison with other techniques represents the most suitable approach.

Except for our group's recent work on voidage and particle velocity measurements [1,3], there have been few attempts to systematically compare different measurement techniques in the past. Werther et al. [4] compared solid velocity measurements obtained by a laser doppler anemometer (LDA) and a single fibre reflection probe in the dilute zone of a circulating fluidized bed riser. These experiments were performed under identical conditions with the same equipment. However, the comparison could not be performed for high-solid-concentration flows since LDA is effective only for dilute suspensions. Panday et al. [5] compared the time-average solid velocity in a CFB obtained by a dual multi fibre optical probe with data obtained by high-speed particle image velocimetry. Good agreement was observed between the results of these two techniques, but the comparison was limited to one operating condition and few locations.

In this study, four different experimental techniques – radioactive particle tracking (RPT) a non-invasive technique available at the Ecole Polytechnique de Montréal, Positron emission particle tracking (PEPT), a non-invasive technique developed at the University of Birmingham, optical fibre probes, an invasive technique deployed at the University of British Columbia (UBC), and borescopic high-speed particle image velocimetry (PIV), an invasive measurement technique owned and operated by Particulate Solid Research Inc. (PSRI) – were employed to investigate particle vertical motion in the travelling fluidized bed (TFB) facility. This equipment and its auxiliaries were designed and built to assure identical operation in different locations where alternative experimental measurement techniques are available.

In this paper, radial profiles of time-average particle velocity and the probability distribution function of solid velocity obtained by all four techniques are directly compared. Particle velocity results obtained from the TFB with fluid cracking catalyst (FCC) particles are presented elsewhere [1]. In this paper, the TFB experiments were performed with a Geldart group B particulate material, sand particles which differed greatly in properties from the group A particles investigated separately [1]. This resulted in a different flow regime and different solid velocity profiles. In particular, for the operating conditions of interest, the sand particles exhibited the square-nosed slugging flow regime typical of Geldart B particles fluidized at superficial gas velocities (U_g) greater than the minimum slugging velocity (U_{ms}), satisfying the criteria for reaching the slug flow regime [6]. This type of slug flow is regarded as a breakdown of proper fluidization, where high pressures and high interstitial flow rates may break up the dense phase regions releasing pockets of gas, resulting in unstable behaviour. This flow regime, mainly observed in laboratory and pilot scale fluidized beds and of interest for few applications [7,8], provides a useful platform for satisfying the main objective of the study, which is to compare

experimental the features of a number of the most advanced particle velocity measurement techniques under identical operating conditions. Analysis of the results, focusing on the physical principles underlying each experimental technique and taking into account global flow structures of the multiphase system, provides valuable insights into the reasons for the observed discrepancies.

2. Experimental

The experimental apparatus consists of the easily-disassembled fluidization column, its support structure, basic instrumentation and auxiliary components, all of which travelled with silica sand (d_{sauter} = 292 μm, ρ_p = 2640 kg/m^3) particles (as well as FCC powder) to different research laboratories for experimentation using different sophisticated instrumentation. The travelling fluidized bed apparatus, shown schematically in Figure 1, features a transparent plexiglass column of 0.96 m length × 0.133 m i.d. dense bed section, surmounted by a 1.36 m long × 0.190 m i.d. freeboard section. An internal cyclone with its dipleg terminating in the dense section (0.70 m above the distributor) was employed to capture any entrained particles. Detailed description of the apparatus, and its auxiliary components are given elsewhere [1,9]. Details of the measurement techniques used to determine particle velocity − optical fibre probes, borescopic high-speed PIV, PEPT and RPT − are given elsewhere [1]. Table 1 summarizes the key features of each of these experimental techniques. The optical probe, borescope and RPT solid tracer used in the previous study with FCC powder [1] were used again in this paper for sand.

4

Table 1 – Summary of particle velocity measurements techniques characteristics. In each case, measurements were at 0.24, 0.40 and 0.56 m above the distributor and at superficial gas velocities of 0.40, 0.50 and 0.60 m/s. The static bed height was 0.82 m for all cases.

	Borescopic high-speed PIV	Optical fibre probe	RPT	PEPT
Sampling rate	3000 frame/s	15.6 kHz (wall region) 62.5 (other positions)	100 Hz	Variable up to 500 Hz
Sampling period	10 s (10×1 s intervals)	40 s (80×0.5 s intervals)	8 h (2×4 h)	3.5 h (3×1 h + 1×0.5 h)

The minimum fluidization velocity of the sand particles was 0.0796 m/s [9], and all the operating superficial gas velocities investigated were less than U_c (0.72 m/s), the superficial gas velocity corresponding to onset of the turbulent fluidization flow regime, obtained from pressure fluctuation data [3,9], and above U_{ms} (0.16 m/s), the minimum slugging velocity, calculated from the correlation of Stewart and Davidson [6]. As visually observed from X-ray images [10], typical of Geldart B particles [11] in smooth-walled columns of high *H/D*, the sand particles exhibited square-nosed slugging behaviour, with dense plugs occupying the entire cross-section of the bed moving upwards and solids raining from the bottom through the slug.

The tracer used for the PEPT study with sand differed from that used for FCC powder in order to better match the physical properties of the bulk solids. Sand particles could not be activated enough for the PEPT experiments. Therefore, aluminum oxide, in super-activated base form (gamma-alumina) with properties given in Table 2, was used as the tracer particle. The size and shape of this tracer particle matched well the bulk solid mean diameter, but its density was higher. The RPT tracer particle differed in shape, diameter and density from the sand particles, as shown in Table 2. Considering the sensitivities of the systems when the experiments were performed, the tracer particles employed for both RPT and PEPT represented the best available

substitutes for sand particles. For the RPT and PEPT experiments, a single tracer particle was added to the system and its motion followed by the detectors.

Table 2 – Comparison of key physical properties of bed material and RPT and PEPT tracer particles

	Sand	PEPT Tracer	RPT Tracer
Composition	99.9% SiO_2	γ-Al_2O_3	Pure scandium dipped in epoxy
d_{sauter} (µm)	292	300	400
ρ_p (kg/m^3)	2640	3000	2000
shape	Irregular	Irregular	Nearly spherical
U_t (m/s)	0.73	0.91	2.35
Radioactivity (mCi)	0	1.34 (1st day) 0.60 (2nd day)	0.20

The sand particles were white, producing bright images without proper contrast in the borescopic imaging, resulting in poor particle boundary distinction. Antipolar filters mounted on the borescope window did not improve the image quality. The best solution in terms of the image contrast was achieved by colouring all the particles using a dark red PSRI proprietary dye. Application of this dye did not appreciably alter the particle diameter or density.

The same data analysis techniques as were described by Tebianian et al. [1] for the FCC particles, were employed for the sand particles.

3.   Results

3.1   Radial profiles of time-average particle velocity

Radial profiles of time-average particle velocity obtained by all four experimental techniques are reported in Figures 2 to 4. Axial symmetry is assumed in each of these figures. As for FCC particles [1], the results from the borescope, PEPT and RPT results in these plots only include velocity vectors associated with solid motion with a deviation angle with respect to the vertical

6

direction of 30 degrees or less. As for FCC particles [1], considering each measurement level, the time-averaged particle velocity profiles have been determined by considering the average velocity obtained from the motion of all particles moving almost vertically in a specific radial location, without distinguishing whether they were moving in the dense plug or the dilute region, given that the simultaneous voidage data are not obtainable from particle tracking techniques. The measurement locations of the optical probe and the borescope were points along a diameter of the bed while for RPT and PEPT the measurements were obtained in five concentric areas into which the cross-section was divided. The radial positions of PEPT and RPT particle velocity profiles correspond to the centres of these concentric annuli. The error bars for the RPT, borescope and optical fibre probe represent 90% confidence intervals, obtained by considering the whole sample of velocity vectors in the time series data recorded during the measurement period for each measurement location. For PEPT, since the location precision was available for each instantaneous tracer position, the uncertainty in the solid velocity was determined using the same error propagation formula as for FCC powder [1].

The solid raining associated with the square-nosed slug flow regime produced, mainly for the upper sections of the column, an unusual trend, with pronounced negative time-average solid velocity at all radial positions. However, although the measured velocities were mostly negative, solids flux data [12] indicate that the upward and downward mass fluxes averaged over time and the cross-section were in balance, as expected when entrainment fluxes are low.

For U_g = 0.40 m/s, the results obtained by RPT, the optical probe and borescopy are in good qualitative and quantitative agreement at the lowest measurement level (z = 0.24 m), where these three techniques provide downward solid velocity near the wall and upward velocities in the centre of the bed, typical of bubbling fluidized beds (Figure 2). The poorest agreement between

7

the results was observed at 0.40 m above the distributor plate where a quasi-flat radial profile was observed for all four techniques due to the uniform upward motion of particles in the dense plugs and downwards motion resulting from particles raining in the slugs, with PEPT providing the most negative values, RPT and borecope results close to zero, and the optical probe results in the middle. For all three measurement levels, the profiles obtained by RPT and borescopy are quite close to each other, as shown in Figure 2.

For $U_g = 0.50$ m/s, agreement among the results of the borescopy, RPT and optical probe at the lowest measurement height is slightly worse than for $U_g = 0.40$ m/s, where some signs of downward solid velocity in the core region are observable from the optical probe radial profile. At the upper measurement section ($z = 0.56$ m), there is poor agreement among the results in the wall region relative to the central region where the profiles obtained by all four techniques were closer to each other. Similar behaviour to that shown in Figure 2 for $z = 0.40$ m was observed for $U_g = 0.50$ m/s in Figure 3, where PEPT produced negative values of greater magnitude than the other three techniques for most cases.

For $U_g = 0.60$ m/s (Figure 4), radial profiles of solid velocity at $z = 0.24$ and 0.40 m presented similar behaviour as described for $U_g = 0.50$ m/s. At the upper measurement level, solid raining in the central region of the bed was less prominent compared to the two lower superficial gas velocities investigated.

Since the optical fibre probe detects only the vertical motion of particles, the data were also analyzed by averaging the vertical component of all velocity vectors of particles that cross the measurement level for the borescope, PEPT and RPT (i.e. by removing the restriction of diverging by ≤30° from the vertical). However, except for a few cases in Figure 5 (comparable to

8

the Figures 2 and 3 results at the lowest measurement level), there was no significant change in the results, suggesting that contributions from non-vertical particle velocities were minimal.

3.2   Probability distribution function of solid velocity

Probability distribution functions (PDF) of the instantaneous solid velocity measured at different positions obtained by each measurement technique are plotted in Figure 6. All four techniques detected particles raining inside the slugs, giving bimodal PDFs. The optical probe and PEPT detected downward velocities of greater magnitude than RPT and the borescopic high-speed PIV, especially in the middle section of the column ($z = 0.40$ m). PEPT, borescopy and optical probe detected similar upward velocities, whereas RPT presented more wide-ranging data, i.e. more prominent "tails".

Figure 7 shows instantaneous movement of the particles in the central region of the bed captured by the optical probe and the borescope. The sampling time consisted of ten periods of 1 s duration for the borescope and 80 periods of only 0.5 s duration for the optical probe. Continuous data capture giving a complete picture of the slugging phenomena and the raining phenomenon was not possible in either case. Nevertheless, the plots still portray the intermittency of upward velocities associated with the roof and floor regions of slugs interspersed with downward motion caused by particles raining inside the voids. Note that the actual time intervals between successive bursts (random for the optical probe and 5.67 s for the borescopy) are not represented in the plots in order to facilitate the visualization of the slugging phenomena.

The presence of the slugs for sand particles was further confirmed by the pressure fluctuation data in Figure 8, with the frequency confined to a narrow range of lower frequencies, more characteristic of slug flow, than for the FCC particles. The differential pressure was measured at

9

different 0.16 m-height sections of the column. The zero-magnitude pressure drop observed regularly for sand particles corresponds to the passage of the square-nosed slugs covering the entire section across which the differential pressure transducer was measured. It can be observed that unlike FCC powder, for sand particles the pressure drop was zero for almost 1 s, indicating that the slug heights exceeded the height of the measurement interval of the pressure transducers. The pressure fluctuations data of FCC powder reported in Figure 8 confirm the presence of a more chaotic flow regime typical of turbulent fluidization, as reported in the previous study [1].

Figure 9 represents the instantaneous velocity of the tracer particle passing the level 0.56 m above the distributor for both RPT and PEPT. PEPT shows a higher density of upward velocities, with an almost constant value and more scattered downward velocities characterized by bigger magnitudes. RPT, as indicated also in the PDFs, presents more symmetrical velocity vectors with respect to zero and a smaller count frequency than PEPT.

4. Discussion

Consideration of the unique characteristics of each of the four measurement techniques, taking into account the presence of square-nosed slugging flow regime, helps to explain the quantitative differences in the data yielded by these four advanced methods. Factors which have contributed, at least in part, to the differences include:

- The optical probe and borescopic probe are both intrusive, and therefore interfere to some extent with the flow field being measured. The degree of interference depends on factors such as the probe shape, size and orientation, velocity and void fraction of the local gas-solid flow [10].

10

- The PEPT and RPT methods rely on the tracer particle travelling in a manner that is identical to the other particles in the bed. However, as seen in Table 2, the shape, diameter and density of the tracer particle used for RPT differed substantially from those of the bulk particles, with the tracer particle being considerably larger and less dense. This was the best tracer particle available with RPT system when these experiments were performed. However, note that the RPT tracer preparation method has been improved since then, with the ability to produce tracer particles with properties closer to those of the bed material. For the PEPT measurements, the tracer particle size and shape were well matched, but its density was higher. These differences in particle properties may have affected the measurements, e.g. influencing velocity fluctuations and acceleration, thereby preventing the tracer from faithfully representing the behaviour of the bed material. Particle tracking techniques require close matching of all three key particle physical properties (size, shape, density) for accurate determination of particle motion by following the motion of a tracer particle. Note also that an ideal radioactive tracer particle only represents a single average size and density of the sand particles; whereas the optical probe and borescope measure the velocities of all particles present in the bed. The terminal velocity (U_t) of the RPT and, to a lesser extent, PEPT tracer particles in air was greater than that of the bulk sand particles. However, the terminal velocity only accounts for a combination of tracer density and diameter (slightly more important) given in the drag coefficient expression. As reported by Rowe and Nienow [13], the density difference is considerably more important than the size difference in determining solid segregation in gas-fluidized beds. The tracer particles employed in the RPT and PEPT experiments differed significantly in terms of density which can produce different circulation patterns, regardless of the degree of similarity of

11

terminal velocities. In fact, as shown in Figure 9, the count frequency, defined as the number of times the tracer particle was detected in a certain region over the entire sampling time, obtained by PEPT was more than twice that of RPT. One reason leading to this could have been less "mobilization" of the RPT tracer particle, possibly due to its greater diameter. Sand particles may also have abraded the tracer particles modifying their shape during the operation of the system.

- The sampling rate of the RPT system was fixed and equal to 100 Hz, whereas the PEPT detection rate was variable and could reach rates as high as 500 Hz. Suppose that the tracer displacement during time-steps Δt_1 and Δt_2 are $\overline{\Delta x_1}$ and $\overline{\Delta x_2}$, respectively, where $\Delta t_1 + \Delta t_2 = \Delta t = 10$ ms. RPT detects the mean tracer movement associated with Δt given by $(\overline{\Delta x_1} + \overline{\Delta x_2})/\Delta t$, whereas PEPT can detect two velocity vectors $\overline{\Delta x_1}/\Delta t_1$ and $\overline{\Delta x_2}/\Delta t_2$. Generally $(\overline{\Delta x_1} + \overline{\Delta x_2})/\Delta t \neq mean(\overline{\Delta x_1}/\Delta t_1, \overline{\Delta x_2}/\Delta t_2)$. This difference may result in different velocities evaluated by PEPT and RPT. Note that recent modifications in RPT system mean that higher sampling frequencies could now be achieved.

- As reported in Tables 1 and 2, tracer radioactivity, detection instrumentation and the localization algorithm employed by the two particle tracking techniques (RPT and PEPT) differed substantially, possibly resulting in different detected tracer velocities over the sampling time as shown in Figure 9.

- The average resolution of the PEPT system given by location uncertainty was between 2.7 and 4.3 mm for different runs, which was of the same order as the distance travelled by the particle during one time step at low velocities (< 0.06 m/s). This may have resulted in poor

accuracy when detecting low solid velocities. Instantaneous location uncertainty of RPT data was not available, but RPT applied to systems similar to the TFB [14] presented a spatial resolution of around 6 mm, which may lead to similar lack of accuracy.

- The four methods have different dependencies on particle volume fraction, as discussed in our previous work [1]. The PIV algorithm used to analyse the borescopic images requires a sufficient number of particles in the measurement volume for accurate velocity determination [15]. Detection of the movement of solids far from the borescope tip is challenging due to loss of focus. The velocities measured by the optical probe can be considered to be "volume-fraction-independent" since, in a given time interval, a particle velocity is returned irrespective of the number of particles passing in the correct direction during that interval. On the other hand, in the RPT and PEPT methods, over a certain time period, the tracer particle spends more time in regions of high flux than in low-flux regions. Therefore, RPT and PEPT are "flux-dependent".

- The Fast Fourier Transform (FFT) analysis performed on the time-series of pressure fluctuations of the system suggests a dominant frequency in the range of [0.40-0.43 Hz] for passage of slugs, as shown for example in Figure 8, corresponding to a time-interval between arrival of slugs of 2.3 to 2.5 s, though with surrounding peaks of higher frequency. The time interval between successive acquisitions (of duration of 1 s) was 5.67 s for the borescopy, i.e. one measurement every 6.67 s. This may have led to some aliasing in the borescope data, with successive measurements tending to favour one phase. The optical probe data did not present the same aliasing issue since its data were captured randomly over a longer sampling period. RPT and PEPT data samplings were continuous for long periods of time, again preventing the aliasing problem.

13

- Raining of particles inside the slugs (extremely dilute region) played a prominent role in the determining the values of time-average solid velocity (Figures 7 - 9). Negative particle velocities in the interior of the column are detected more accurately when flux-independent or concentration-independent measurement techniques encounter such flows. It can observed that there is significantly better agreement between the results of RPT, borescopy and optical probe in the lower region of the bed where the slugs have not yet formed and upward movement of the particles in the middle of the bed is dominant (rising with bubble noses and wakes). The profiles obtained by all four techniques are closer in the upper region than in the middle section ($z = 0.40$ m). This could be due to the presence of the cyclone dipleg terminating at $z = 0.70$ m that could have contributed to slug break-up and reduced particle raining [9].

5.   Conclusion

Radioactive particle tracking, positron emission particle tracking, optical fibre probe and borescopic high-speed PIV were deployed to investigate local particle velocities in a novel traveling fluidized bed operated under identical experimental conditions with sand particles (a Geldart Group B powder). Significant quantitative differences were observed among the radial profiles of time-average velocity provided by the four techniques, especially in the middle section of the bed. Likely reasons for these differences include invasiveness of two of the methods, differences between the physical properties of the tracer and sand particles, differences in sensitivity to the concentration of particles in the measurement zone, spatial resolution of the particle tracking systems and differences in measurement volumes. The analysis of the data gives valuable insights into the features of each measurement technique.

14

The scatter of the data, especially in the middle section, limits the usefulness of these results as benchmarks for CFD validation. However, direct comparison of the results provides useful information for the future deployment of these techniques in the investigation of particle velocities in gas-fluidized beds.

Acknowledgement

Nomenclature

D Column diameter, m

d_{sauter} Sauter mean particle diameter, μm

H Static bed height, m

U_c superficial gas velocity at transition to turbulent fluidization flow regime, m/s

U_g superficial gas velocity, m/s

U_{ms} minimum slugging velocity, m/s

U_t terminal settling velocity in air, m/s

$\overline{\Delta x}$ tracer particle displacement, m

Δt time lag between successive tracer detections, ms

ρ_p solid density, kg/m^3

z vertical coordinate measured from top of gas distrbutor, m

Acronyms

FCC   fluid cracking catalyst

FFT   Fast Fourier Transform

PDF   probability distribution function

PEPT   positron emission particle tracking

PIV   particle image velocimetry

PSRI   Particulate Solid Research Inc.

RPT   radioactive particle tracking

TFB   travelling fluidized bed

UBC   University of British Columbia

References

[1] S. Tebianian, K. Dubrawski, N. Ellis, R.A. Cocco, R. Hays, S.B. Reddy Karri, T. W. Leadbeater, D. J. Parker, J. Chaouki, R. Jafari, P. Garcia-Trinanes, J. K. Seville, J. R. Grace, Investigation of particle velocity in FCC gas-fluidized beds based on different

measurement techniques, Chem. Eng. Sci. 127 (2015) 310–322. doi:10.1016/j.ces.2015.01.049.

[2] J. Werther, Measurement techniques in fluidized beds, Powder Technol. 102 (1999) 15–36. doi:10.1016/S0032-5910(98)00202-2.

[3] K. Dubrawski, S. Tebianian, H. T. Bi, J. Chaouki, N. Ellis, R. Gerspacher, R. Jafari, A. Kantzas, C. Lim, G. S. Patience, T. Pugsley, M. Z. Qi, J. X. Zhu, J. R. Grace, Traveling column for comparison of invasive and non-invasive fluidization voidage measurement techniques, Powder Technol. 235 (2013) 203–220. doi:10.1016/j.powtec.2012.10.031.

[4] J. Werther, B. Hage, C. Rudnick, A comparison of laser Doppler and single-fibre reflection probes for the measurement of the velocity of solids in a gas-solid circulating fluidized bed, Chem. Eng. Process. Process Intensif. 35 (1996) 381–391. doi:10.1016/0255-2701(96)80018-3.

[5] R. Panday, L.J. Shadle, M. Shahnam, R. Cocco, A. Issangya, J.S. Spenik, et al., Challenge problem: 1. Model validation of circulating fluidized beds, Powder Technol. 258 (2014) 370–391. doi:10.1016/j.powtec.2014.02.010.

[6] P.S.B. Stewart, J.F. Davidson, Slug flow in fluidised beds, Powder Technol. 1 (1967) 61–80. doi:10.1016/0032-5910(67)80014-7.

[7] I.W. Noordergraaf, A. Van Dijk, C.M. Van Den Bleek, Fluidization and slugging in large-particle systems, Powder Technol. 52 (1987) 59–68. doi:10.1016/0032-5910(87)80007-4.

[8] I.C. van Putten, M. van Sint Annaland, G. Weickert, Fluidization behavior in a circulating slugging fluidized bed reactor. Part I: Residence time and residence time distribution of polyethylene solids, Chem. Eng. Sci. 62 (2007) 2522–2534. doi:10.1016/j.ces.2005.10.025.

[9] S. Tebianian, Comparison of Alternative Advanced Experimental Techniques for Measurement of Hydrodynamic Characteristics of Gas-Fluidized Beds, PhD disseration, University of British Columbia (2015).

[10] S. Tebianian, N. Ellis, P. Lettieri, J.R. Grace, X-ray imaging for flow characterization and investigation of invasive probe interference in travelling fluidized bed, Chem. Eng. Res. Des. In press (2015). doi:10.1016/j.cherd.2015.08.006.

[11] W.-C. Yang, Bubbling Fluidized Beds, in: W-C. Yang (Ed.), Handbook of Fluidization and Fluid-Particle Systems, Marcel Dekker, Inc., New York, (2003).

[12] S. Tebianian, K. Dubrawski, N. Ellis, R.A. Cocco, R. Hays, S.B. Reddy Karri, T. W.

Leadbeater, D. J. Parker, J. Chaouki, R. Jafari, P. Garcia-Trinanes, J. K. Seville, J. R. Grace, Comparison of alternative solids flux measuring techniques in fluidized beds, Submitted for publication (2015).

[13] P.N. Rowe, A.W. Nienow, Particle mixing and segregation in gas fluidised beds. A review, Powder Technol. 15 (1976) 141–147. doi:10.1016/0032-5910(76)80042-3.

[14] M. Rasouli, RPT Error Position, Personal Communication (2014).

[15] M. Raffel, C. Willert, J. Kompenhans, Particle Image Velocimetry, A Practical Guide Springer, N. Y. (1998).

List of Figures

Figure 1 – Schematic diagram of travelling fluidized bed apparatus: a) assembled; b) exploded modular view. Adapted from Tebianian et al. [1]

Figure 2 – Radial profiles of time-average solid velocity at three levels for sand, $U_g = 0.40$ m/s

Figure 3 – Radial profiles of time-average solid velocity at three levels for sand, $U_g = 0.50$ m/s
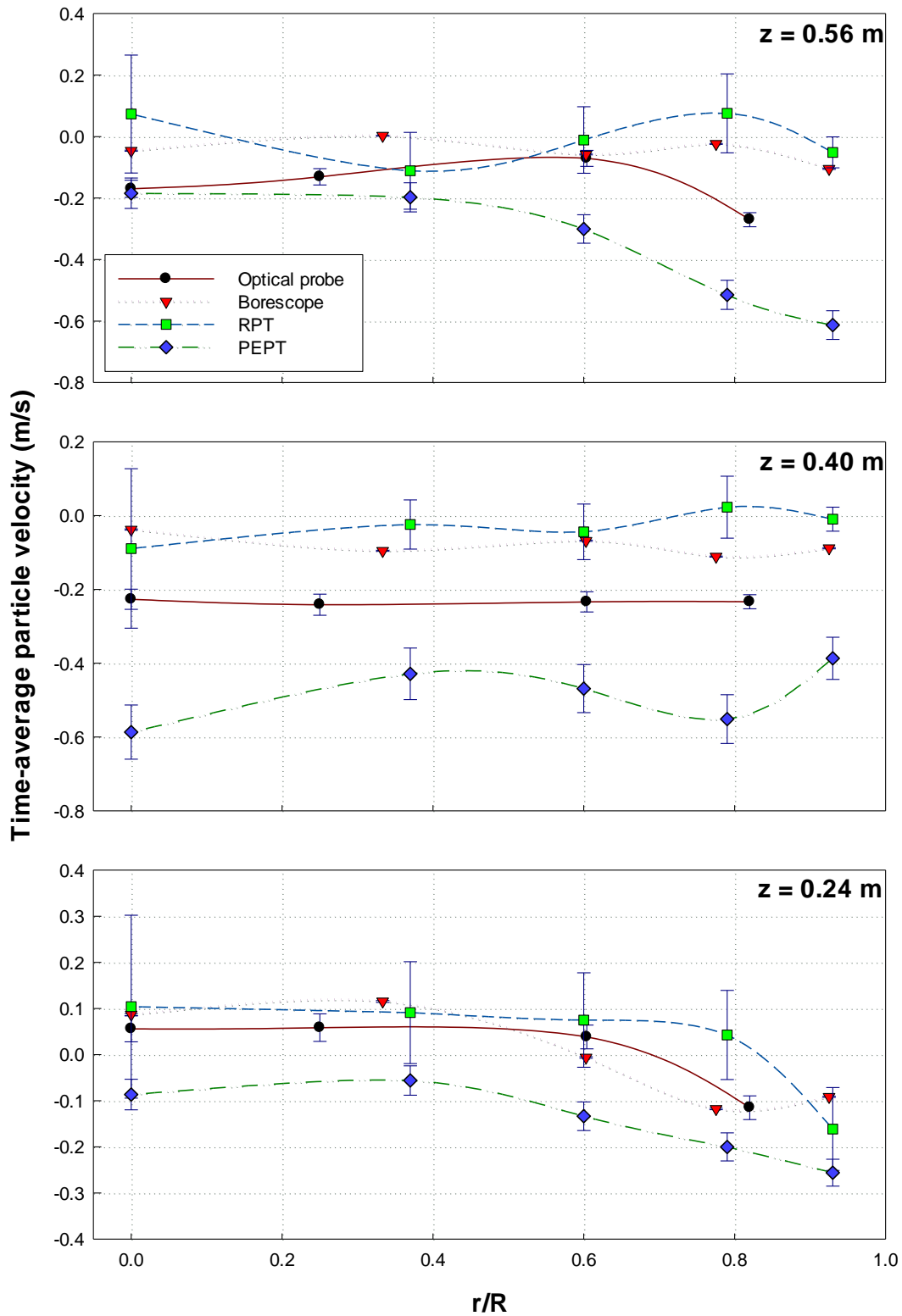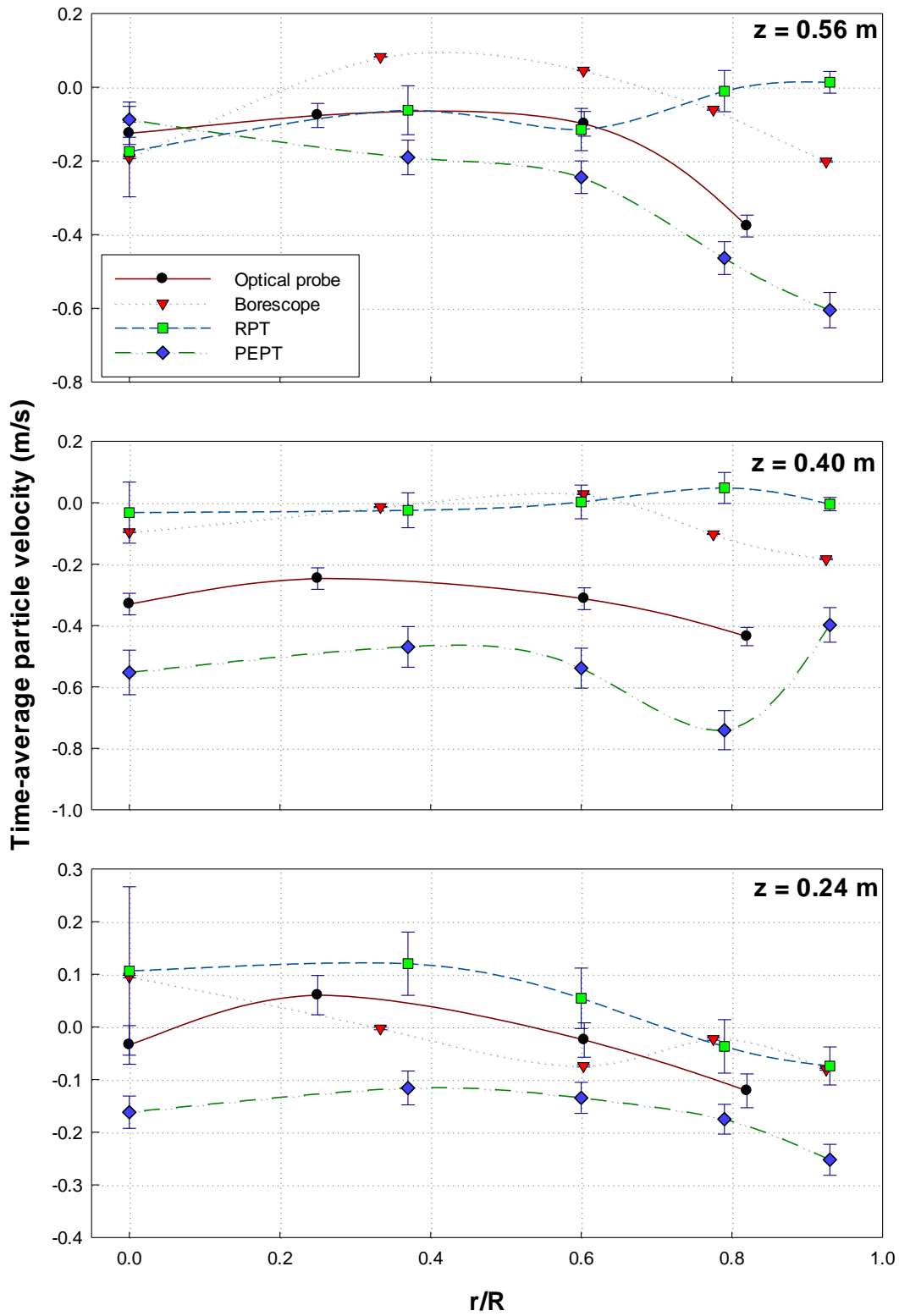
Figure 4 – Radial profiles of time-average solid velocity at three levels for sand, $U_g = 0.60$ m/s

Figure 5 – Radial profiles of time-average solid velocity at three levels for sand based on vertical components of velocity vectors

Figure 6 – Examples of probability distribution function of solid velocity

Figure 7 – Solid velocity time series obtained by: a) Optical probe; b) Borescope. Note that the traces are not continuous, but broken into bursts of duration 1s for the borescope and 0.5 s for the optical probe.

Figure 8 – Pressure fluctuation data and FFT analysis for sand and FCC particles at $U_g = 0.50$ m/s between z = 0.24 and z = 0.56 m. Expanded bed height was 1.17 m.

Figure 9 – PEPT and RPT tracer velocity crossing the level $z = 0.56$ m during the entire sampling period

(a)   (b)

Internal cyclone

Freeboard

Dense bed section

Figure 1 – Schematic diagram of travelling fluidized bed apparatus: a) assembled; b) exploded modular view. Adapted from Tebianian et al. [1]

Figure 2 – Radial profiles of time-average solid velocity at three levels for sand, U_g = 0.40 m/s

Figure 3 – Radial profiles of time-average solid velocity at three levels for sand, $U_g = 0.50$ m/s
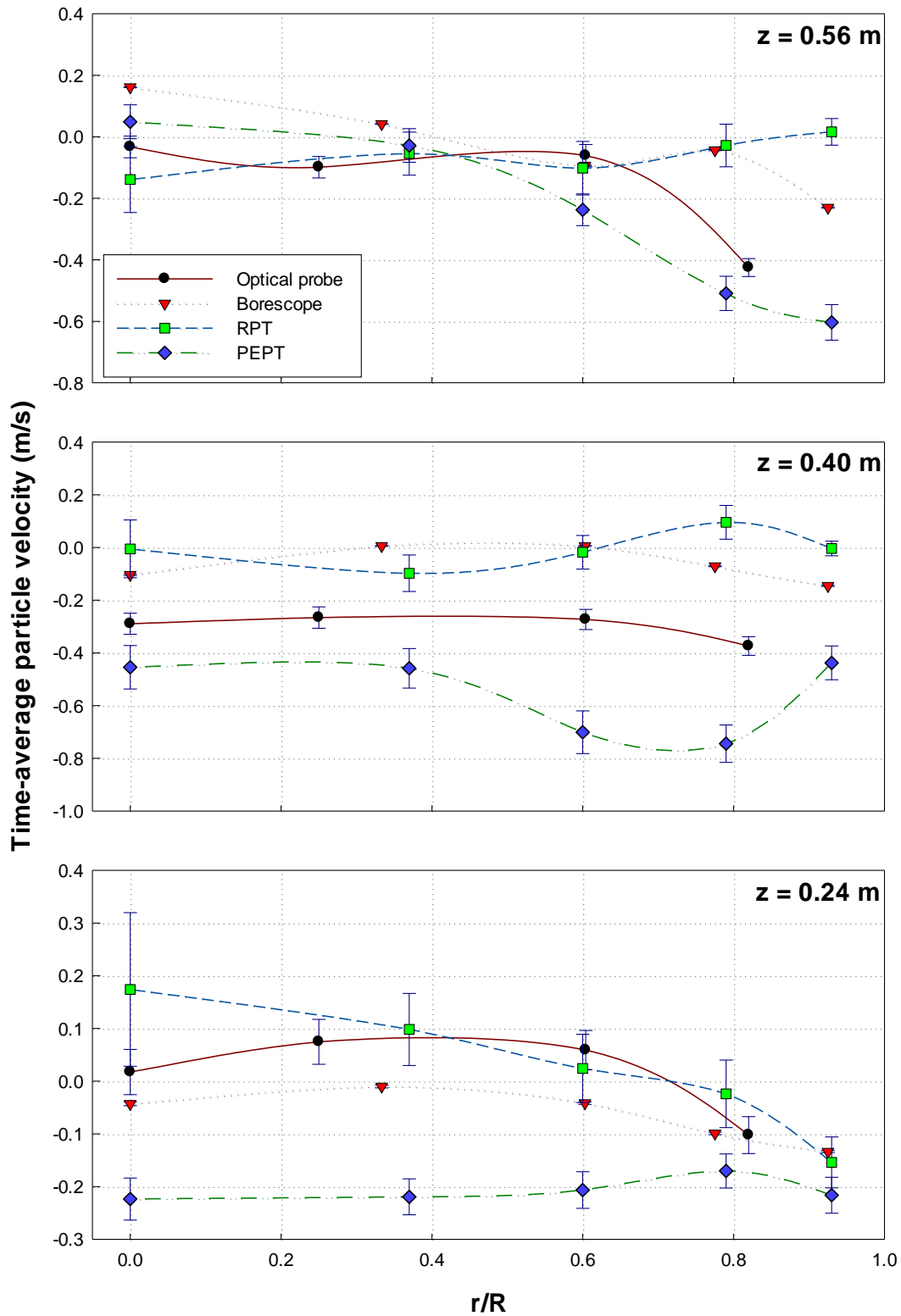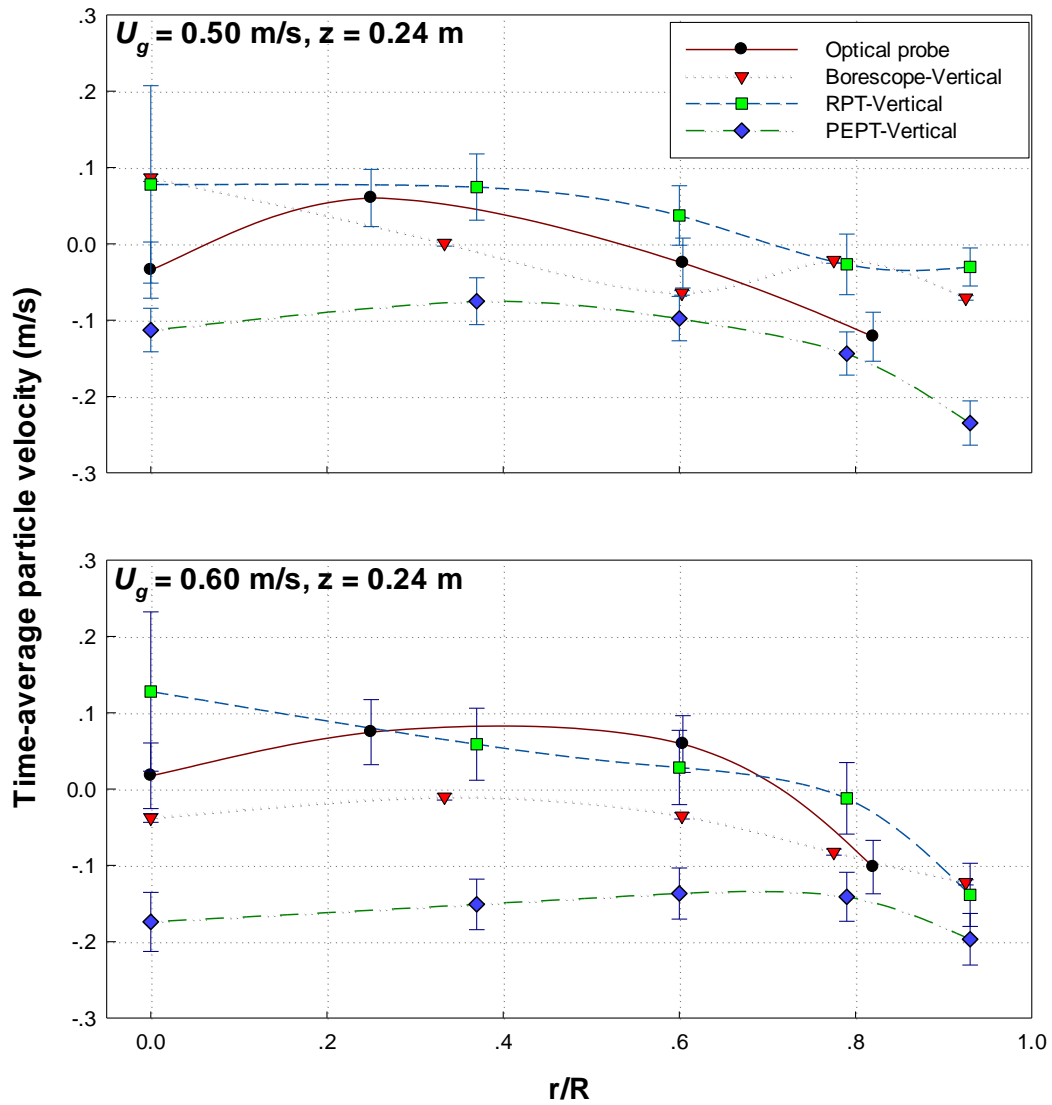
Figure 4 – Radial profiles of time-average solid velocity at three levels for sand, $U_g = 0.60$ m/s

Figure 5 – Radial profiles of time-average solid velocity at three levels for sand based on vertical components of velocity vectors
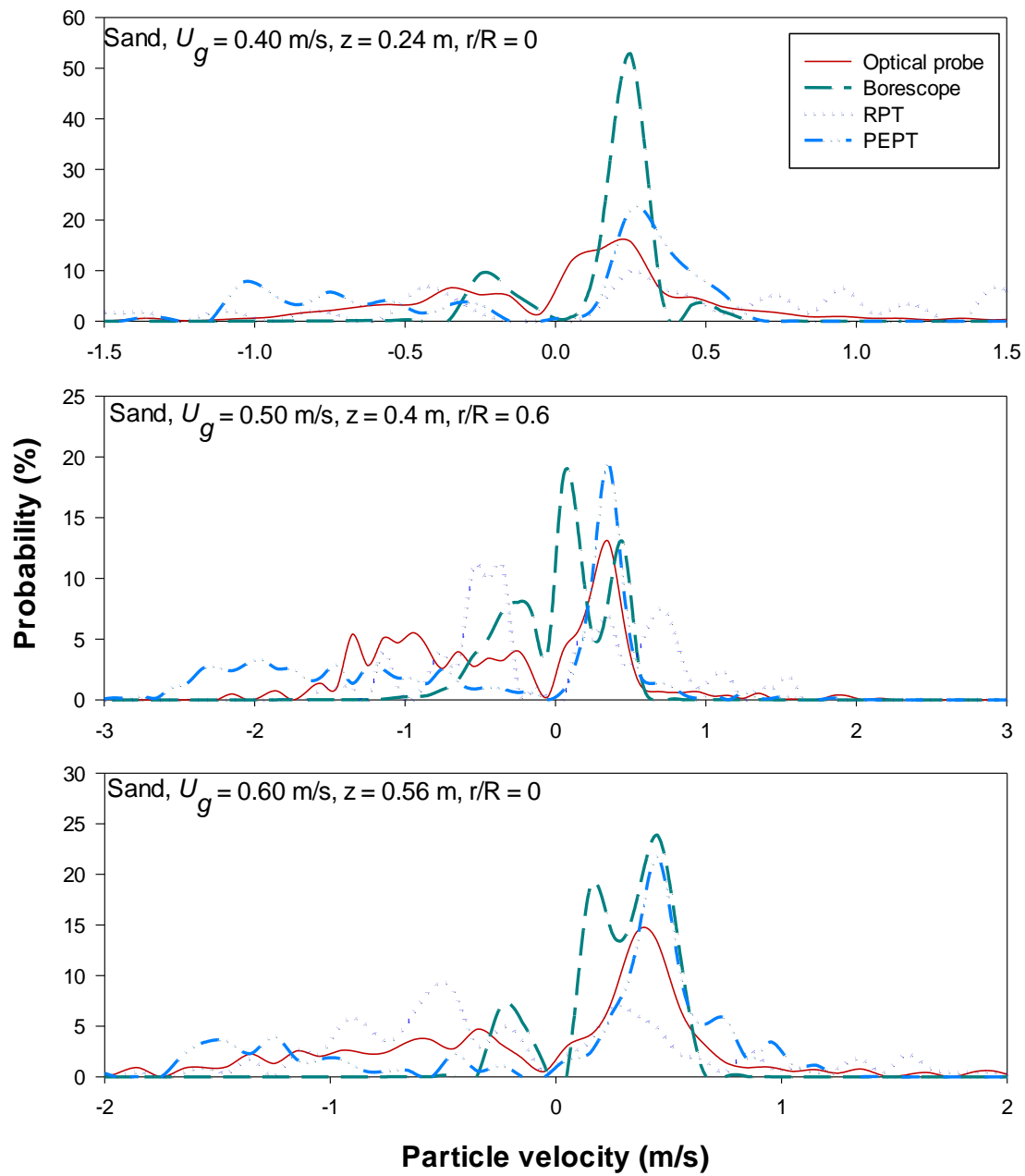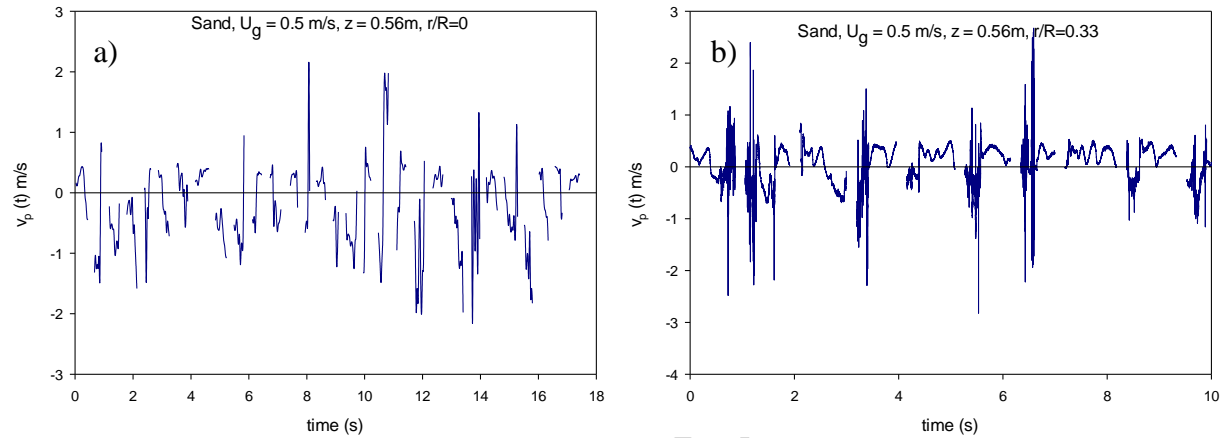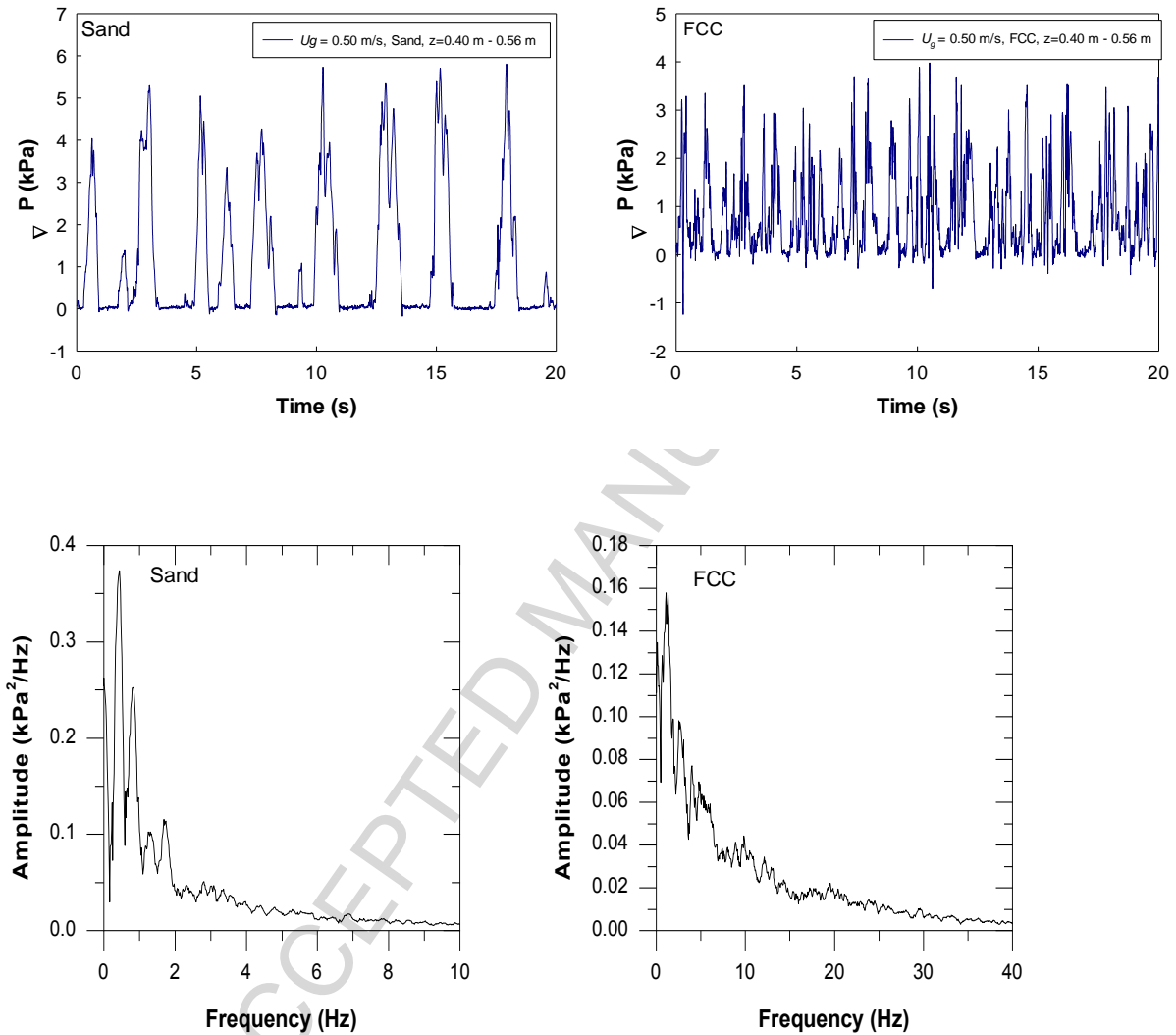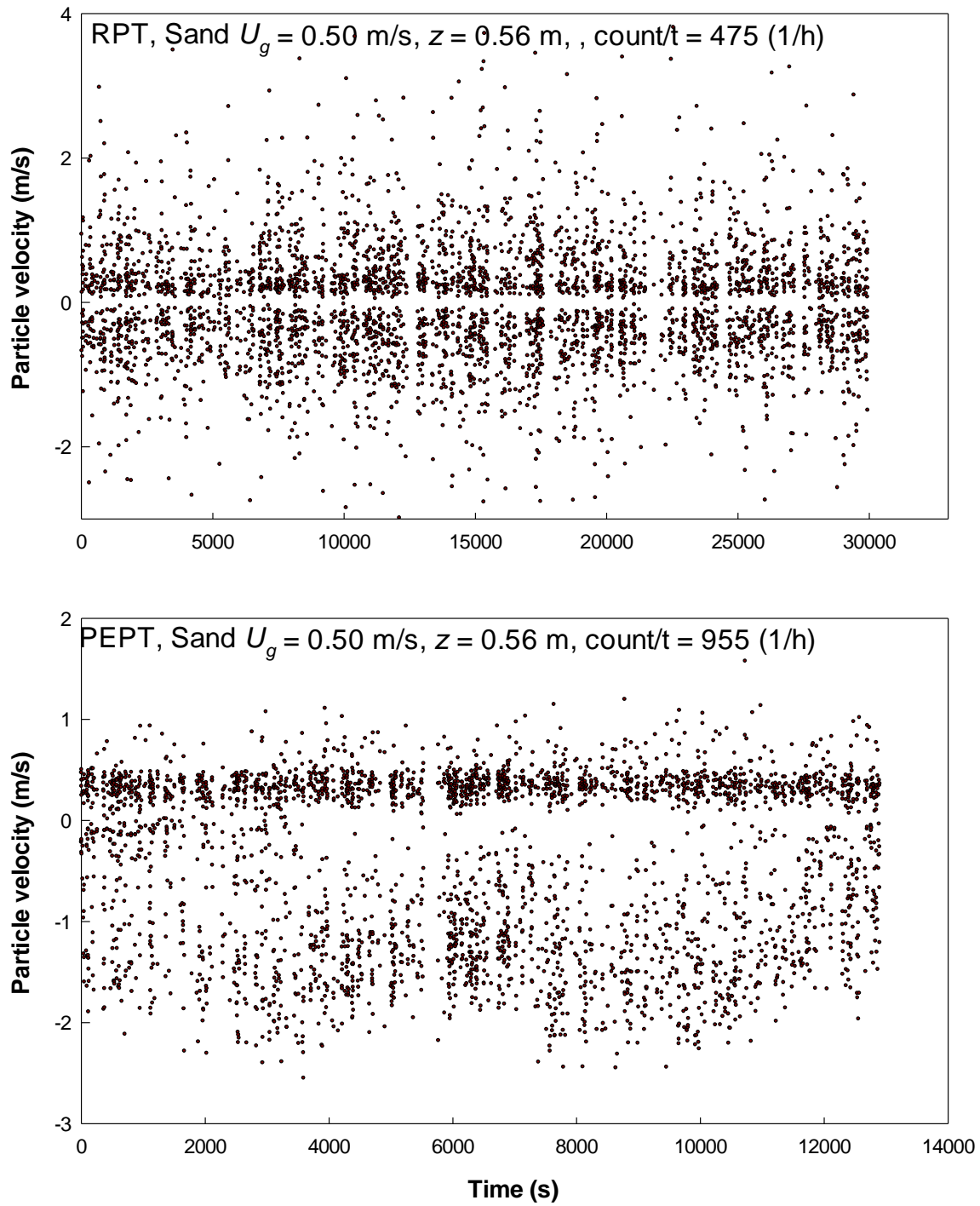
Figure 6 – Examples of probability distribution function of solid velocity

Figure 7 – Solid velocity time series obtained by: a) Optical probe; b) Borescope. Note that the traces are not continuous, but broken into bursts of duration 1s for the borescope and 0.5 s for the optical probe.

Figure 8 – Pressure fluctuation data and FFT analysis for sand and FCC particles at U_g = 0.50 m/s between z = 0.24 and z = 0.56 m. Expanded bed height was 1.17 m.

Figure 9 – PEPT and RPT tracer velocity crossing the level $z = 0.56$ **m**
during the entire sampling period

The travelling fluidized bed, operating under identical conditions at different research laboratories, was employed to compare particle velocity profiles, obtained by advanced measurement techniques (RPT, PEPT, borescopy and optical probe), for sand particles in square-nosed slugging regime. The results provide valuable insights on the features of each measurement technique.

Graphical abstract

Highlights

- Identical operating conditions were achieved in different locations
- The hydrodynamics of the square-nosed slugging flow regime were investigated
- Advanced particle velocity measurement techniques give different results
- The reasons for the observed discrepancies among the results are explored